Universiteit Leiden
The Netherlands

Optimization of quantum algorithms for near-term quantum computers

Bonet Monroig, X.

6. Quantum simulation of hydrogen molecule on Quantum Inspire

6.1. Introduction

In the last decade the field of quantum computation has experienced an unprecedented expansion due to the development of better and larger quantum computer prototypes. Such developments have brought the attention of governments and companies with the aim of transferring academic knowledge into impactful applications for society. One of the first consequences of such effort has been the appearance of publicly accessible quantum computers via cloud services. This has allowed researchers world-wide to be able to perform their own quantum computations without the need of a specialized laboratory.

An increase in size and quality of quantum hardware is expected in the upcoming years. However, these devices will fall within the noisy intermediate-scale quantum [47] (NISQ) paradigm. It still remains an open question whether NISQ hardware will be able to achieve some level of beyond classical computation. For this reason, it is expected that the main users of cloud-based quantum computing services will be researchers with the goal of exploring how quantum computers can speed-up relevant academic and industrial problems. Therefore, the upcoming generation of cloud-based quantum computers should take into the needs of these researchers.

One of the first public quantum computers *Quantum Inspire* was made available in The Netherlands in a collaboration between TU Delft and TNO [181, 182]. The goal of *Quantum Inspire* is to provide users access to various technologies to perform quantum computations and insights in principles of quantum computing and access to the community [181]. The current version of *Quantum Inspire* allows users to use its simulator, a 5-qubit superconducting quantum processor (Starmon-5) device and a 2-qubit spin qubit processor (Spin-2).

Performing a quantum computation with quantum hardware requires a high level of knowledge and expertise. Fortunately, existing cloud-based quantum computers are built with user-friendly interfaces such that running small experiments is possible with average coding skills. While these simplifications allow anyone to access quantum computers, they typically have a negative impact on the quality and flexibility of the algorithms that can be run on them. In this work we use *Quantum Inspire* a to calculate the dissociation curve of the Hydrogen molecule (H_2). Our goal is to explore the limits of *Quantum Inspire* for running NISQ computation, assessing the quality of the results, and the potential time overhead associated with interaction between local computers from users and the cloud-based service.

6.2. Quantum simulation of the Hydrogen molecule

6.2.1. Variational quantum eigensolvers

In the upcoming years it is expected that quantum hardware will be limited to a few hundreds of moderate quality qubits, with stringent limitations in coherence time and gate fidelities. To overcome such difficulties, variational quantum eigensolvers (VQE) were designed to combine quantum and classical resources such that the potential of noisy qubits is maximized. A VQE uses a quantum processor to prepare a parametrized quantum state $|\psi(\vec{\theta})\rangle$ and measure a quantum observable $\hat{O}$ such that

$$\langle O\rangle = \langle\psi(\vec{\theta})|\hat{O}|\psi(\vec{\theta})\rangle. \tag{6.1}$$

The expectation value of the observable serves as a cost function to a classical optimization loop that suggests new parameters. This process is repeated until some convergence criteria is met. The quantum state $|\psi(\vec{\theta}_{\text{opt}})\rangle$ is an approximation to the lowest eigenstate of the observable, and respectively its expectation value is an approximation to its lowest eigenvalue. To run a VQE on real quantum hardware, one must prepare the parametrized quantum state through a quantum circuit. Within this quantum circuit, some of the gates have the possibility to be continuously changed through a classical knob $U(\vec{\theta})$ such that

$$|\psi(\vec{\theta})\rangle = U(\vec{\theta})|\psi_0\rangle, \tag{6.2}$$

where $|\psi_0\rangle$ is an initial quantum state (i.e. $|0\rangle^{\otimes N}$, Hartree-Fock, Gaussian state, etc.).

6.2.2. Ground-state energy of the Hydrogen molecule via VQE

The hydrogen molecule (H_2) has become a standard benchmark problem to solve using near-term quantum hardware. Calculating the ground-state energy using a VQE has done extensively in the past years [39, 41, 42, 44, 45, 83, 98]. The number of qubits required to compute the ground-state energy of this problem in its minimal basis (STO-3G) is 4. However, one can further reduce the problem to 2 qubits by removing qubits from the inherent symmetries of the problem. Following ref. [41] we use the 2-qubit Hamiltonian under the Bravyi-Kitaev transformation at different bond distances R,

$$H(R) = h_0(R)II + h_1(R)ZI + h_2(R)IZ + h_3(R)ZZ + h_4(R)XX + h_5(R)YY, \tag{6.3}$$

where the coefficients h_i also dependent on R. Their values can be efficiently computed using standard quantum chemistry packages [89, 90].

It is possible to obtain the exact ground-state energy of our target problem with a single parameter quantum circuit. In fig. 6.1 we show the quantum circuit implemented to calculate the ground-state energy of the problem by optimizing the free parameter θ. The parametrized part of the circuit is constructed from the unitary operation

$$U(\theta) = e^{-i\theta X_0 X_1}, \tag{6.4}$$

and decomposed into a circuit by standard methods [31] (see boxed region in fig. 6.1). The circuit is initialized in the Hartree-Fock state $|\psi_0\rangle = |10\rangle$ using a π-rotation around the y-axis. A final phase correction is needed to find the correct solution ($\frac{\pi}{2}$ rotation around the z-axis) which is implemented virtually. The final single-qubit gate rotations are used to measure the different Pauli operators of the Hamiltonian 6.3.

6.2.3. Implementation in Quantum Inspire

We use the infrastructures provided by *Quantum Inspire* [181] to calculate the dissociation curve of the H_2 molecule with the Starmon-5 processor. While *Quantum Inspire* provides a user-friendly web interface we code the quantum circuits with the Software Development Kit (SDK). The circuits are then uploaded to a server and are automatically scheduled and executed. After the completion of the experiment we receive a dataset with a binary shot count for every circuit. The data is downloaded to a local computer, processed to obtain the expectation values of every

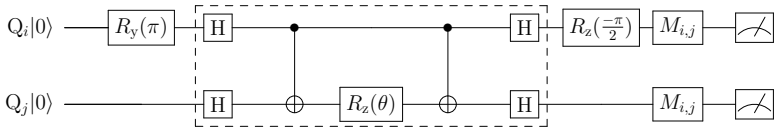

Figure 6.1.: Quantum circuit used to calculate the ground-state energy of the H_2 molecule. There is an optimal value of θ such that the circuit reaches the exact ground-state energy of the Hamiltonian in eq. 6.3 for every bond distance R.

operator in eq. 6.3, and added to obtain the final energy. The fact that the data must be locally processed makes it nearly impossible to run an optimization algorithm to optimize the angle. Instead of running the VQE algorithm with the quantum hardware, we obtain the optimal angles from a classical simulation of the perfect algorithm. These optimal angles are implemented in the Starmon-5, using different combination of qubit pairs, as well as simulating them with sampling and measurement error.

Our goal is to run the circuit from fig. 6.1 with the optimal parameters previously obtained. However the actual circuit executed at the hardware level might not be exactly the one we upload to the server because there might be gates that are not native to the hardware. In our experiment we use two qubits of the Starmon-5 device available in *Quantum Inspire*. The Starmon-5 device does not have CNOT and H as native gates, thus they are automatically decomposed onto native gates. Despite the fact that we do not know the exact decomposition, we can make an estimate on the total circuit time following the specifications from the gate time specifications in [181],

$$t_{\text{cir}} = 3 \cdot t_{1\text{q}} + 2 \cdot t_{\text{H}} + 2 \cdot t_{\text{CNOT}} + t_{\text{meas}} + t_{\text{init}} \tag{6.5}$$

$$= 3 \cdot 20 + 2 \cdot 40 + 2 \cdot 100 + 2000 + 150 \sim 2500 \text{ ns}. \tag{6.6}$$

Those gates that are not native to Starmon-5 are automatically decomposed into native gates. As we do not know exactly which decomposition takes place we have assumed that $t_{\text{H}} = 40$ ns and $t_{\text{CNOT}} = 100$ ns. These numbers are taken from the fact that a generic single-qubit gate takes 20 ns and a two-qubit gate takes 60 ns, so we assumed two single-qubit gates to decompose a H-gate, and two single-qubit gates and a two-qubit

to decompose a CNOT.

In order to calculate the cost function of the problem, in our case the energy from the Hamiltonian 6.3, we must prepare and measure the state multiple times. Additionally, it is not possible to measure all terms of the Hamiltonian simultaneously, therefore each cost function evaluation requires to prepare N different circuits to estimate all the operators. In our experiments we measure every operator with its own circuit, thus needing a total of six circuits per evaluation. Every circuit is then measured with $M = 2^{12}$ shots. An estimate total time T for a single function evaluation is the

$$T = t_{\text{cir}} \cdot \text{M} \cdot \text{N} \sim 2.5 \cdot 2^{12} \cdot 6 = 61440\mu s = 61.44 \text{ ms}. \tag{6.7}$$

However the number we obtained above does not reflect the actual runtime of a single function evaluation. There are time-delays associated with communication to the server, as well as periodical calibration and tune-up steps running in the background from which the user has no control. Therefore the total wall-time of running a single experiment is much longer than expected. In our result we studied the actual wall-clock time that takes to run a single function evaluation of the H_2 molecule.

6.2.4. Results

The results of running the optimal angles on the *Quantum Inspire* infrastructure are shown in fig. 6.2. A first observation is that the simulated results with sampling noise match almost perfectly the exact ground-state energy curve. However when one includes measurement errors in the simulation the energy error increases to 0.6 to 0.7, showing how much impact this has on the accuracy of the algorithm (dashed green curve). By applying measurement corrections the energy error is reduced by almost an order of magnitude in the simulations (dashed red curve).

Turning our attention to the curves computed with the Starmon-5 device we observe a remarkable feature that the same qubit pair with different order does not result in an identical or even similar curve. For example, the pink and light blue curves are obtained using the qubits 1 and 2, but they when qubit $i = 1$ is used the results are up to 6 times worse than when $i = 2$. An exact same trend is observed when the qubits picked are 0 and 2 (brown and green curves). Such an asymmetric behavior of the system with the same qubit pair might be explained by the large differences in coherence times and gate fidelities between qubits. When the qubit with the worst parameters carries the majority of the gates, such

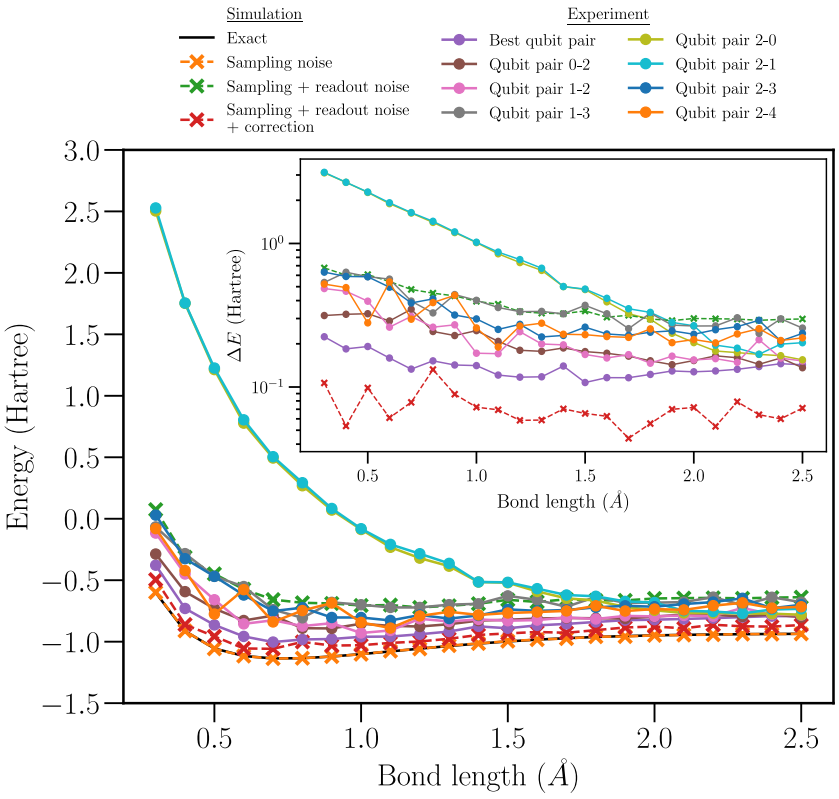

Figure 6.2.: Approximate ground-state energy and energy error ΔE (inset) of the H_2 molecule with respect to the bond distance. The solid black line depicts the exact ground-state energy dissociation curve of the problem. Classically simulated energy and energy errors are shown in dashed lines with a cross marker. We simulated three types of errors: sampling noise, sampling noise with measurement errors and sampling noise with measurement and a correction to the measurement error. Energies computed with the quantum device are shown in solid lines with a dot marker. Each curve represents the result of the experiment implemented on a different pair of qubits from the Starmon-5.

a large difference in performance is not surprising. A similar asymmetry is observed when the pair of qubits 2 and 4 is used (purple and orange curves), although it is less pronounced. One possible reason for the less pronounced asymmetry is the fact that these qubits are the best pair in the device as described in the characterization data in ref. [181].

Perhaps the most striking result is given by the qubit pair 1 and 3 (grey curve). We would have expected to see a much worse result in the dissociation curve in this combination because qubits 1 and 3 are not directly coupled, and qubit 2 must be involved to mediate the interaction (see ref. [183] for details of the chip). An additional number of single- and two-qubit gates is required to implement our circuit 6.1 using qubits 1 and 3, and therefore a much worse performance is to be expected. One potential explanation is that *Quantum Inspire* automatically re-assigned the qubit pair to a pair that is directed interacted. Unfortunately, it is not possible for the end-user to know in more detail what happens after the job is submitted to the server.

We are also interested in obtaining the real runtime of performing the experiments on a cloud-based system. For this, we extracted the wall-clock time used to obtain every point in the dissociation curve for every qubit pair used. In figure 6.3 we depict the runtime for every point of the dissociation curve for every qubit pair. For each qubit pair we also calculate the mean and standard error of all the times. In average the total runtime per point is between 85 to 90 seconds. Compared to the estimated runtime from eq. 6.5 of 61.4 milliseconds, it represents more than 4 orders of magnitude in runtime. While our estimation did not include communication delays and other related times, it is surprising that all of them amount to more than a minute long.

We also observe three points that required more than 100 seconds to compute. A reason for them to occur might be because a characterization step took place in between the execution of the computation. Such process occurs periodically and automatically and the end user has no control or knowledge that it has occurred. This is particularly worrisome as the parameters of the device might suddenly change while the computation is not finished, thus making the computational unreliable.

6.3. Conclusion and outlook

Quantum computers promise a computational advantage compared to classical computers for specific problems. In the past decade world-wide efforts from public and private entities have produced a significant num-

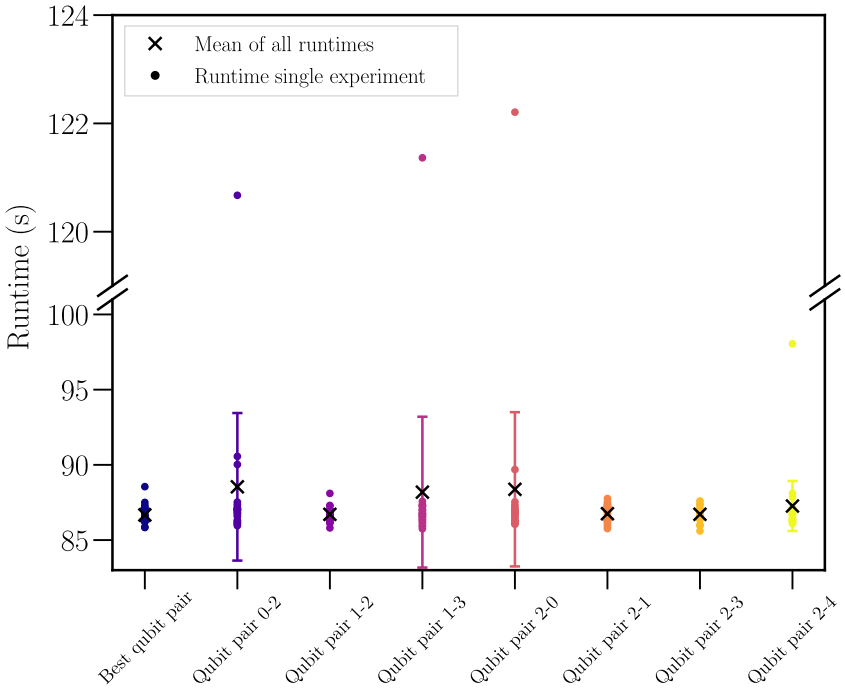

Figure 6.3.: Runtime of calculating every point in the dissociation curve (dots) for each qubit pair. The cross for every qubit pair represents the mean time of all points calculated with that qubit pair, the associated error bar is the the 95% confidence interval of the population.

ber of prototypes of quantum computers, yet requiring expensive and specialized equipment that only few laboratories can maintain. Even though the state-of-the-art quantum hardware is not yet at the point where unambiguous quantum advantage can be proved, they serve as a test-bed for researchers to explore their potential. To engage with more researchers some of these laboratories with quantum computer prototypes have opened their resources to the public through cloud-access. In this chapter we explore capabilities of one of such platforms *Quantum Inspire* for research purposes.

Our first result show that even a 2-qubit toy experiment such as the ground-state dissociation curve of the H_2 requires a high level of expertise and knowledge to be performed. First of all, users must be familiar with the programming language of the platform to describe the quantum circuits to be run. Once the quantum program is ready users must upload it to the server, moment at which users have no longer control over the algorithm. In our case we have observed an unexpected good performance from a qubit pair that is not directly coupled. A possible explanation for this result is that the system has automatically implemented the experiment in a different qubit pair. Even though this might be an expected behavior of the system, the providers must carefully specify which actions are taken such that the results are trustworthy.

Secondly we study the runtime of measuring a single point in the H_2 dissociation curve. We show that the time required to obtain this point on the cloud service requires up to 4 orders of magnitude more time than an estimated expected runtime. This is worrisome if one aims at using cloud-based quantum computers for research purposes in the NISQ era. The coherence times of NISQ device is expected to be relatively short, and thus the time required to interact with the hardware must be minimized as much as possible.